molecular pharmaceutics

pubs.acs.org/molecularpharmaceutics Article

The Influence of the Strength of Drug–Polymer Interactions on the Dissolution of Amorphous Solid Dispersions

Kweku K. Amponsah-Efah, Pinal Mistry, Reed Eisenhart, and Raj Suryanarayanan*

Cite This: https://dx.doi.org/10.1021/acs.molpharmaceut.0c00790 Read Online

ACCESS | Metrics & More | Article Recommendations | Supporting Information

ABSTRACT: In an earlier report, ionic interactions between ketoconazole (KTZ), a weakly basic drug, and poly(acrylic acid) (PAA), an anionic polymer, resulted in a dramatic decrease in molecular mobility as well as reduced crystallization propensity of amorphous solid dispersion (ASD) in the solid state. On the other hand, weaker dipole–dipole interactions between KTZ and polyvinylpyrrolidone (PVP) resulted in ASDs with higher crystallization propensity (Mistry et al. *Mol Pharm.*, **2015**, *12* (9), 3339–3350). In this work, we investigated the behavior of the ketoconazole (KTZ) solid dispersions in aqueous media. *In vitro* dissolution tests showed that the PAA ASD maintained the level of supersaturation for a longer duration than the PVP ASD at low polymer contents (4–20% w/w polymer). Additionally, the PAA ASDs were more resistant to drug crystallization in aqueous medium when measured with synchrotron X-ray diffractometry. Two-dimensional ^{1}H nuclear Overhauser effect spectroscopy (NOESY) NMR cross peaks between ketoconazole and PAA confirmed the existence of drug–polymer interactions in D_2O. The interaction was accompanied by a reduced drug diffusivity as monitored by 2D diffusion ordered spectroscopy (DOSY) NMR and enthalpy-driven when characterized by isothermal titration calorimetry (ITC). On the other hand, drug–polymer interactions were not detected between ketoconazole and PVP in aqueous solution, with NOESY, DOSY, or ITC. The results suggest that interactions that stabilize ASDs in the solid state can also be relevant and important in sustaining supersaturation in solution.

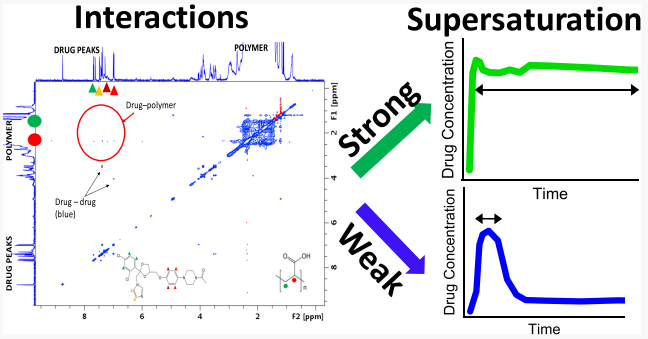

KEYWORDS: *ketoconazole, amorphous solid dispersion, drug–polymer interactions, ITC, NMR, NOESY, DOSY, dissolution apparatus IV, synchrotron X-ray diffractometry, crystallization*

INTRODUCTION

The rate and extent of drug absorption following oral administration is influenced by solubility in the gastrointestinal (GI) fluid and permeability through the GI membrane.[1] Advances in combinatorial chemistry and high-throughput screening methods have led to an increase in target specificity and hydrophobicity of drug candidates.[2,3] With more than 70% of drugs under development having high permeability but poor aqueous solubility (BCS Class II compounds), strategies that enable increased apparent aqueous solubility have become important.[1,4] One strategy is to use amorphous solid dispersions (ASDs), which refer to molecular-level mixtures of drug and polymer, formulated with the aim of improving oral bioavailability. From a formulation perspective, the first step toward stabilization of ASDs is to prevent drug crystallization in the solid state during storage, and polymers have proven effective in that regard.[5] The ability of the polymer to increase the glass transition temperature (T_g) of the dispersion,[6] to reduce molecular mobility,[7] and to act as a physical barrier to molecular aggregation[8−11] have all been linked to crystallization inhibition in the solid state.

If the drug is retained in the amorphous state until used by the patient but crystallizes rapidly following oral administration, the potential solubility advantage may be negated. Adequate supersaturation in the GI fluid must be maintained for a period long enough to translate to enhancement in absorption and consequently bioavailability. Therefore, in addition to stabilizing the drug in the dry solid dispersion, polymers must help maintain drug supersaturation in solution. To gauge the extent and duration of solubility enhancement, amorphous formulations are usually evaluated using *in vitro* dissolution tests. The physicochemical properties (such as the degree of lipophilicity and ionizability) of both the polymer and the drug, viscosity of the diffusion layer, the drug-to-polymer ratio of the formulated ASD, and the nature and strength of drug–polymer interactions are all key factors that

Received: July 29, 2020
Revised: November 17, 2020
Accepted: November 17, 2020

can influence the degree of supersaturation and the drug concentration in solution as a function of time.

The strength of intermolecular interactions can be rank-ordered as ionic interactions > hydrogen bonding > dipole−dipole (non-specific) interactions.[12] Several studies have highlighted a general correlation between the strength of drug−polymer interactions and the physical stability of ASDs upon storage.[13−17] Strong drug−polymer interactions may prevent drug crystallization in the solid state by increasing miscibility, improving phase homogeneity, and/or decreasing molecular mobility.[13,17−19] In an aqueous environment, however, the role of the type and strength of drug−polymer interactions on the dissolution enhancement is not as clear. On the one hand, it is believed that, when the strong solid-state interactions persist in aqueous solution, the initial dissolution rate of the drug increases, and the level of supersaturation is sustained for a much longer duration.[20] Specific interactions that are resistant to disruption by water molecules would thus be most beneficial. On the other hand, it has also been suggested that strong solid-state drug−polymer interactions may be detrimental to ASD performance in aqueous solution. As an example, drug−polymer hydrogen bonding in the solid state was posited to cause a reduction in the dissolution rate for ASDs with low polymer content.[21] There is a need for studies that comprehensively characterize interactions in the solid state as well as in aqueous solutions to enable rational selection of polymers during the development of ASDs.

We demonstrated, in an earlier report, that the weakly basic drug ketoconazole (KTZ) exhibited ionic as well as strong hydrogen bonding interactions with poly(acrylic acid) (PAA) when formulated as an ASD.[13] As a result, there was a dramatic reduction in the molecular mobility of the system and a consequent reduction in crystallization rate, both in the supercooled[13] and glassy states.[22] In contrast, poly(2-hydroxyethyl methacrylate) (PHEMA) and polyvinylpyrrolidone (PVP) showed weaker hydrogen bonding and dipole−dipole interactions with KTZ, respectively. The strength of drug−polymer interactions, reduction in molecular mobility, and the enhancement in physical stability followed the same rank order: PAA > PHEMA > PVP. The pronounced physical stabilization afforded by PAA raised the question: Is the KTZ−PAA interaction, observed in the solid state retained in aqueous medium following dissolution of the dispersion? If so, does the interaction prolong supersaturation? To extend our work, we hypothesize that strong drug−polymer interactions in the solid state can translate to interactions in solution, thereby facilitating sustained supersaturation.

Our first objective was to evaluate the performance of the amorphous dispersions in aqueous media. Two complementary approaches were taken. (i) *In vitro* dissolution tests provided a measure of the drug concentration in solution and the duration of supersaturation. (ii) The extent of drug crystallization as a function of time, monitored following wetting of the dispersion, provided a measure of the ability of the dispersion to resist crystallization. Our second objective was to identify and characterize the drug−polymer interactions in aqueous solution. Two-dimensional nuclear Overhauser effect spectroscopy (2D-NOESY) was used to probe the spatial proximity of drugs and polymers in solution.[23] The impact of interactions on drug diffusivity was assessed with diffusion ordered spectroscopy (DOSY).[24−27] Finally, the thermodynamic "binding" signature and the strength of the interactions were measured with isothermal titration calorimetry (ITC).[28]

EXPERIMENTAL SECTION

Materials. Crystalline ketoconazole was obtained from Laborate Pharmaceuticals (Haryana, India). PAA ($M_w \approx 1800$ g/mol) was purchased from Sigma-Aldrich (Missouri, USA), PVP-K12 ($M_w \approx 2000-3000$ g/mol) was obtained from BASF (New Jersey, USA), and PHEMA ($M_w \approx 3700$) was obtained from Polymer Source (Quebec, Canada). All solvents and chemicals were of analytical grade. The structures of all the compounds used are given in Figure 1.

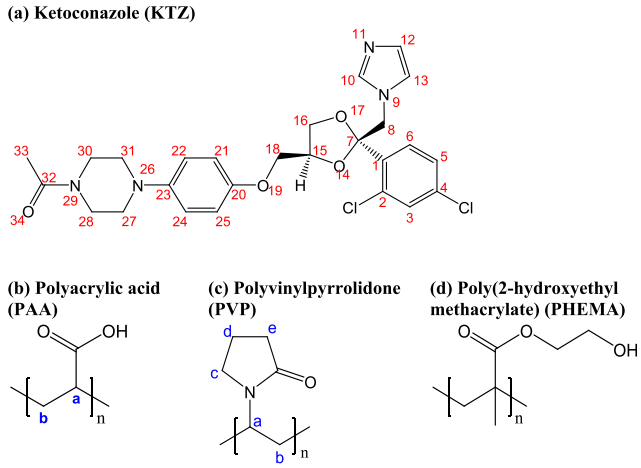

Figure 1. Structures of the (a) model drug (KTZ) and (b−d) polymers (PAA, PVP, and PHEMA).

Preparation of Amorphous Systems. Neat amorphous KTZ was prepared by melting crystalline KTZ at 160 °C and rapidly cooling in liquid nitrogen. The glass was gently ground using a mortar and pestle to obtain the free-flowing powder. Solid dispersions of KTZ with polymer contents ranging between 4 and 40% w/w were prepared by solvent evaporation followed by melt-quenching. The drug and polymer were dissolved in methanol, and the solvent was rapidly evaporated (IKA-HB10 digital system rotary evaporator, Werke GmbH and Co., Staufen, Germany) at 50 °C under reduced pressure. The powder was further dried under reduced pressure at room temperature for ∼24 h to remove residual solvent before melt-quenching. As controls, physical mixtures were prepared by geometrically mixing neat amorphous KTZ with each polymer (4−40% w/w polymer content). All powders were sifted through 250 μm pore-size sieves before use. Additional details of the preparation methods as well as baseline characterization of the samples by differential scanning calorimetry, infrared spectroscopy, thermal gravimetric analysis, and Karl Fischer titration have been reported elsewhere.[13,29]

***In Vitro* Powder Dissolution Testing.** Dissolution tests were conducted in aqueous phosphate buffer (pH 7.4), using a flow-through cell with a 22.6 mm internal diameter (USP Apparatus 4, Sotax Ltd.) attached to a UV analyzer (Specord 210 Plus). A glass bead (5 mm diameter) was placed at the bottom of the cell to prevent the powder from entering the inlet tubing. The bottom cone of the cell was filled with 1 mm diameter glass beads. A glass microfiber filter (Whatman, 25 mm diameter, 0.7 μm pore size) prevented the undissolved powder from escaping from the top of the cell.

An accurately weighed quantity of the powder sample (50 mg drug equivalent) was distributed throughout the 1 mm glass beads of the flow-through cell. The dissolution medium,

https://dx.doi.org/10.1021/acs.molpharmaceut.0c00790
Mol. Pharmaceutics XXXX, XXX, XXX−XXX

maintained at 37 °C, was pumped through the cell at a flow rate of 4 mL/min. The flow-through cell was operated in the open-loop mode, wherein fresh dissolution medium from the reservoir continuously passed through the cells. At pre-determined time points, the UV absorbance of the filtered sample was measured in line at 225 nm, against a reference cell containing the blank dissolution medium. The absorbance readings were converted to dissolved drug concentration values using a calibration curve.

Experiments were run in triplicate, and the mean and standard deviation values (as error bars) are presented. From each concentration−time dissolution profile, the area under the curve from the start of experiment to the last time point $(AUC)_{(0\rightarrow t)}$, the maximum concentration (C_{max}), and the time to reach the maximum concentration (T_{max}) were determined. The ratio [$AUC_{(0\rightarrow t)}$, sample]/[$AUC_{(0\rightarrow t)}$, crystalline KTZ] was used to quantify the extent of dissolution enhancement. The dissolution enhancement factors were compared using the Student's *t*-test. A *p* value of ≤0.05 was used to assess statistical significance. All dissolution data analyses were performed with OriginLab software.

Synchrotron X-ray Diffractometry. Approximately 20 mg of each sample was accurately weighed in a DSC pan (T-zero, TA Instruments, DE), and 25 μL of phosphate buffer (pH 7.4) was added to uniformly wet the sample. The pan was hermetically sealed, mounted on a custom-made holder, and exposed to synchrotron radiation at pre-defined time intervals for approximately 4 h. Measurements were performed in triplicate using fresh amorphous sample for each run. Details of the experimental setup and data analyses procedures were presented earlier.[29] Diffraction patterns are presented as one-dimensional scattering intensity (I) versus scattering wave-vector ($Q = 4\pi \sin\theta/\lambda$) plots, where θ is the angle of incidence and λ is the wavelength. The crystallinity at each time point was quantified using eq 1, where I_c is the intensity of the crystalline contribution (total area of all crystalline peaks) and I_a is the intensity of the amorphous contribution (area of the amorphous halo).[30] The peak areas were obtained by profile fitting (Jade, Materials Data Inc., CA):

$$\text{crystallinity index} = \frac{I_c}{I_c + I_a} \tag{1}$$

Solution NMR. *Sample Preparation for Solution NMR Experiments.* Two methods were used to prepare drug−polymer mixtures for the NMR experiments. In the first method, an accurately weighed amount of polymer was dissolved in D_2O. The polymer solution (1 mL) was then added to an excess of KTZ (~20 mg) in a glass vial, shaken in a vortex mixer at room temperature for approximately 40 min, filtered (0.45 μm PTFE filter), and transferred to 5 mm NMR tubes for data acquisition. The concentration of KTZ in the filtrate was confirmed by HPLC (USP 25 Assay method for Ketoconazole Solution).

In the second approach, D_2O acidified to pH 2.5 with concentrated hydrochloric acid was used as solvent. Stock solutions of ketoconazole and each polymer were separately prepared in the solvent. Aliquots of the drug and polymer stock solutions were pipetted into a vial and diluted with an appropriate amount of solvent, such that the final drug and polymer concentrations were 5 and 20 mg/mL, respectively. Spectra of the drug−polymer mixtures prepared using both methods were qualitatively similar, except for minor differences that could be explained by expected solution pH variations. Data presented within the text are from the second method of preparation.

As controls, spectra of the neat drug and neat polymer solutions in acidified D_2O were also acquired. Of note, KTZ did not dissolve in D_2O (with or without organic co-solvents) at concentrations high enough for detection. PHEMA was also not soluble in D_2O at relevant concentrations.

One-Dimensional Proton Nuclear Magnetic Resonance Spectroscopy (1D ^{1}H NMR). 1D ^{1}H NMR experiments were performed on either a Bruker Avance III HD 500 MHz two-channel spectrometer equipped with a 5 mm Prodigy TCI cryoprobe with *z*-axis gradients in the magnet or on a Bruker AV 400 spectrometer. Spectral assignments were made based on standard 2D methods such as COSY, HSQC, and HMBC experiments (data not shown) and compared with published data for KTZ,[31,32] PVP,[25] and PAA.[33] Spectra were processed with the Bruker Topspin software (version 3.2).

Two-Dimensional Proton Nuclear Overhauser Effect Spectroscopy (^{1}H^{1}H NOESY). Experiments were performed on a Bruker Avance III HD 500 MHz two-channel spectrometer equipped with a 5 mm Prodigy TCI cryoprobe with *z*-axis gradients in the magnet. Spectra were recorded using standard NOESY pulse sequence with water suppression using excitation sculpting from the Bruker pulse-program library. All measurements were carried out at ambient temperature, ~25 °C. In a typical experiment, data were acquired with 2048 data points in F2, 256 increments in F1, and 16 scans per increment over a spectral width of 12 ppm, with a NOE mixing time of 1 s and a relaxation delay of 2 s. Data analysis was done with the Topspin 3.2 software package.

Two-Dimensional Diffusion Ordered Spectroscopy (2D DOSY). Experiments were performed on a Bruker Avance III (500 MHz) instrument with a 5 mm broadband fluorine observe (BBFO) probe at ambient temperature (~25 °C). The longitudinal eddy current delay bipolar gradient pulse sequence acquired in 2D (ledbpgp2s) was employed for self-diffusion coefficient measurements. Gradient strength was incremented in steps along a linear ramp from 2 to 95% of the maximum strength of ~60 Gauss cm^{-1}. Gradient lengths and diffusion times were optimized for each sample in order to achieve sufficient signal attenuation. The relaxation delay was 2 s, and a total of 16 scans was used for each sample. Data was analyzed with the Topspin 3.2 software. The diffusion coefficient (D) for each species was determined from a fit of selected resonances to eq 2:

$$I = I_0 \times \exp\left[-D \times (2\pi\gamma g\delta)^2 \times \left(\Delta - \frac{\delta}{3}\right) \times 1 \times 10^4\right] \tag{2}$$

where I is the recorded signal intensity as a function of gradient strength g, I_0 is the unattenuated signal intensity, γ is the gyromagnetic ratio of ^{1}H, δ is the length of the gradient pulse (2 ms), and Δ is the diffusion time (~100 ms).

Isothermal Titration Calorimetry (ITC). The objective of the ITC experiment was to obtain a quantitative measure of the drug−polymer interaction strength in aqueous solution. To make this possible, the drug solution concentration had to be high such that an accurately measurable heat (>0.5 μcal, for the largest heat) would be absorbed/released.[34] High KTZ concentrations (40 mM) could be prepared in an acidic solvent (pH 1.1 buffer), but not in neutral buffers.

https://dx.doi.org/10.1021/acs.molpharmaceut.0c00790
Mol. Pharmaceutics XXXX, XXX, XXX−XXX

Sample Preparation for ITC Experiments. KTZ solution (40 mM) was prepared in buffer (pH 1.1 ± 0.1; comprising 106 mM HCl and 50 mM KCl) and filtered (0.45 μm PTFE) immediately before each ITC experiment. Solutions of each polymer (3 mM, calculated based on the weight-average molecular weight of the polymer) were separately prepared using the same buffer (pH 1.1 ± 0.1).

ITC Experiments. Experiments were performed on a Microcal Auto-ITC$_{200}$ system (Malvern Instruments, MA), which has a 200 μL sample cell and an identical reference cell. The sample cell was filled with the polymer solution and titrated with sequential injections of the drug solution at a constant stirring rate of 750 rpm. Control experiments were performed by (i) titrating the drug solution into blank buffer and (ii) titrating the buffer into the polymer solution. Unless otherwise stated, the sample chamber was maintained at 25 °C. The first injection was a 0.4 μL aliquot to remove the effect of solute diffusion across the syringe tip during the equilibration period. This first/initial injection was not considered for analysis. Subsequently, 4 μL injections were made into the sample cell for an experimental run time of 150 min. The duration of each injection was 20 s, and the time interval between successive injections was 180 s. To extend the run time, experiments were performed in an automated "continued injection" mode, wherein, when full, 30 μL of solution was withdrawn from the sample cell and discarded to make room for more sequential injections of the titrant. This process of withdrawing solution from the sample cell and continuing the titrations was repeated for up to six experiments. Microcal origin concat (add-on) software was used to concatenate experiments and to correct for concentration and baseline offsets.

ITC Data Analysis. The heat (Q) measured over time (t) was integrated to obtain the incremental heat ΔQ, which was normalized to the molar concentration of injectant, and plotted as a function of the molar ratio between drug and polymer. Data processing, peak integration, and fitting to the standard binding model was done with the Affinimeter ITC software (Software for Science, Spain).[35] Additional details of the ITC data analysis procedure and the fitting model are provided in the Supporting Information.

RESULTS AND DISCUSSION

Ketoconazole (KTZ, Figure 1a) is weakly basic, with pK_a values of 6.5 and 2.9.[36] As an ionizable compound, KTZ exhibits pH-dependent aqueous solubility, being practically insoluble at pH > 4 but highly soluble in acidic media (pH < 2.5) at room temperature.[36] The speciation profile of ketoconazole, as a function of pH, is given in Figure S1. PAA and PVP are water-soluble over a wide pH range, whereas PHEMA is a "water-swellable" hydrogel with limited aqueous solubility[37] (see Figure 1b–d). The carboxylic acids within the monomer unit of PAA exhibit pH-dependent ionization (pK_a 4.5), being substantially unionized at pH < 2.5 and almost completely ionized at pH > 6.5.[38] PVP, on the other hand, is a relatively "neutral" polymer.[39,40]

In our earlier reports,[13,22] significant differences in the drug–polymer interaction strength, molecular mobility, and the drug crystallization propensity were observed when ASDs formulated with each of the three polymers, at low (4–40% w/w) polymer contents, were characterized. Since low excipient contents in ASDs offer the advantage of reducing the pill burden, it was of interest to evaluate the behavior of the ASDs having such low polymer contents in aqueous media.

Powder Dissolution. Figure 2 shows the dissolution profiles of neat ketoconazole as well as the solid dispersions.

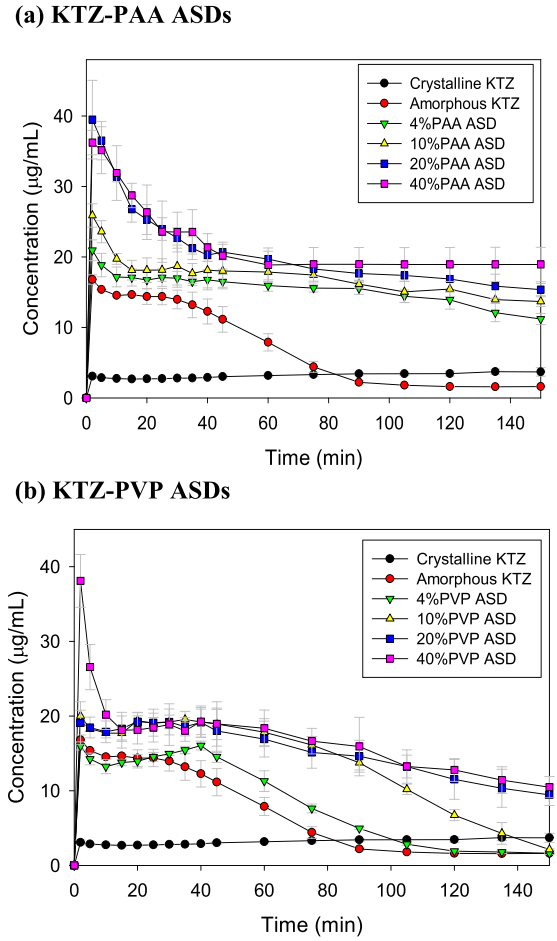

Figure 2. Dissolution profiles of crystalline KTZ, amorphous KTZ, and ASDs formulated with (a) PAA and (b) PVP at polymer contents ranging between 4 and 40% w/w (mean ± standard dev; n = 3). Experiments were performed in pH 7.4 phosphate buffer at 37 °C. Profiles of KTZ–PHEMA ASDs are presented in the Supporting Information (Figure S2a).

Crystalline KTZ yielded a concentration of ∼3 μg/mL in solution, about the same as its reported equilibrium solubility of 2 μg/mL (pH 7.8, 37 °C).[41] Neat amorphous KTZ, however, showed an initial rapid increase in concentration to ∼18 μg/mL, a 6-fold increase compared to the concentration of crystalline KTZ but still far below the estimated "amorphous solubility" of 57 μg/mL (pH 10, 37 °C).[42] The increased drug concentration from amorphous KTZ persisted for approximately 40 min before declining. The rapid increase and decline in concentration are the classical "spring" effect exhibited by amorphous materials in aqueous solution.[43,44]

Dissolution profiles of the PAA ASDs are shown in Figure 2a. At the lowest polymer loading (4% w/w PAA), the drug concentration increased rapidly to ∼20 μg/mL and leveled off with a slight decline. As the polymer content of the dispersion increased (with 10 and 20% PAA), progressively higher maximum drug concentration (C_{max}, see Figure S3a) levels were reached rapidly, though these could not be sustained. The acidic microenvironment created around the weakly basic drug

https://dx.doi.org/10.1021/acs.molpharmaceut.0c00790
Mol. Pharmaceutics XXXX, XXX, XXX–XXX

particles by the rapidly dissolving polymer, PAA, increased the drug solubility, resulting in the high C_{max} values. As recently shown, a 2 to 3 unit decrease in the microenvironmental pH of the dissolving particles could double the initial dissolution rate of KTZ.[45] The high degree of supersaturation however becomes a driving force for crystallization, manifesting as the decline that follows the initial surge in drug concentration.[46] Nonetheless, at all polymer contents, the PAA ASDs maintained ~6-fold higher drug concentration levels by the end of the experimental runs compared to crystalline KTZ. The supersaturation, observed after 40 min, is very likely sustained by a different mechanism since the pH of the dissolution medium in the bulk phase did not reduce significantly (due to the buffer capacity as well as the constant flow of fresh dissolution medium). We hypothesize that drug−polymer interactions in solution will be relevant. Of note, an increase in PAA content from 20 to 40% w/w (Figure 2a) did not translate to any solubility enhancement.

Dissolution profiles of the PVP ASDs, shown in Figure 2b, differ in two main aspects when compared to the profiles of the PAA ASDs. First, the ASDs containing less than 40% PVP do not show the initial spike in drug concentration within the first 40 min. This is understandable since PVP, being a relatively "neutral" polymer, does not lower the pH of the microenvironment of the dissolving drug particles as much as PAA does. Thus, the effect of rapid polymer dissolution driving an increased supersaturation is observed, mainly at higher (>40%) polymer contents. The second general feature identified from the dissolution profiles of the KTZ−PVP ASDs (Figure 2b) is that the drug concentration levels drop after ~40 min, an indication that PVP is not as effective as PAA at inhibiting drug crystallization. The profile of the ASD with 4% PVP content was quite similar to that of neat amorphous KTZ, and a polymer content of at least 20% w/w was required to sustain the KTZ supersaturation for practically useful timescales.

The PHEMA ASDs exhibited slightly different dissolution characteristics (see Figure S2a). The C_{max} values at all polymer contents were not significantly different from the C_{max} of neat amorphous ketoconazole. The level of supersaturation was, however, sustained much longer in the PHEMA ASDs at all polymer contents than in the PVP ASDs. Both effects, i.e., low C_{max} values and the sustained supersaturation, can be explained by the "diffusion-controlled" mechanism of drug release, proffered for ASDs formulated with hydrogels.[47,48] When the ASD is introduced into the aqueous medium, the polymer immediately imbibes water and swells, trapping the drug molecules and preventing the rapid surge in drug concentration, resulting in the low C_{max}. With time, however, the dissolved drug slowly diffuses out of the gel-like polymer matrix at a steady rate, thus sustaining the level of supersaturation.

Selected dissolution profiles of the ASDs are replotted in Figure 3 to enable a better comparison of the polymer effect. Pronounced differences were observed at low polymer contents (4−20% polymer) where supersaturation was sustained for a longer duration in the PAA and PHEMA ASDs.

As controls, binary physical mixtures (PMs) of neat amorphous KTZ and each polymer were subjected to the same dissolution testing experiments (PAA and PVP PMs in Figure 4 and PHEMA PMs in Figure S2b). Generally, at all polymer contents, the physical mixtures achieved similar or even higher C_{max} values when compared to the ASDs (see Figure S3a). Interestingly, the KTZ−PVP physical mixture at

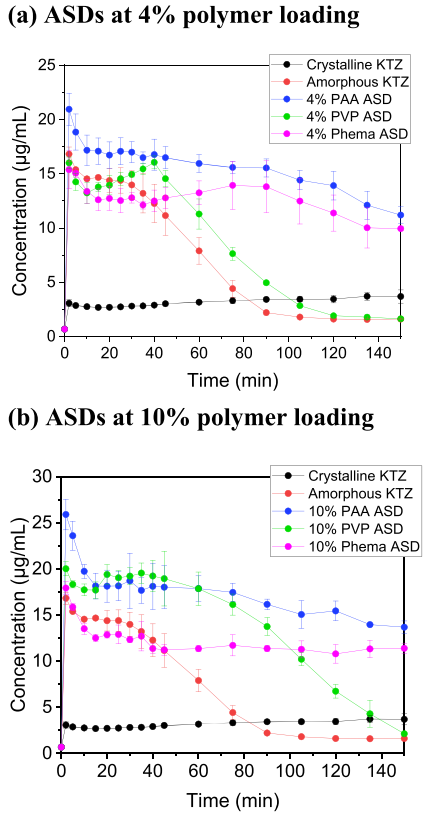

Figure 3. Comparison of dissolution profiles of ASDs formulated at (a) 4% w/w polymer content and (b) 10% w/w polymer content.

40% polymer content showed the highest C_{max} of ~80 μg/mL. In spite of the high C_{max} values, however, the drug concentration levels declined rapidly for all the physical mixtures, regardless of the polymer type. This latter observation is in line with the current state of knowledge that intimate mixing of the drug and polymer at the molecular level greatly helps in sustaining the level of supersaturation.[49,50]

The composite effect of the extent and duration of supersaturation was quantified with the area under the dissolution curve (AUC). The $AUC_{(0\rightarrow 150min)}$ of each formulation was normalized with the $AUC_{(0\rightarrow 150min)}$ of crystalline KTZ, and the resulting dissolution enhancement factors (AUC ratios) are presented in Figure 5. Alternatively, for each sample, the total amount of KTZ dissolved after 150 min is plotted in Figure S3b. The AUC ratios, or the total drug dissolved, allow the dissolution behaviors of the different amorphous systems to be compared. For example, at low (4−20% w/w) polymer contents, the dissolution enhancement from the PAA ASDs was significantly higher than the enhancement from the PVP ASDs. The AUC ratios also allow the effects of polymer type and polymer loading to be compared. A similar level of dissolution enhancement (an AUC ratio of 4.7) could be achieved with either 4% PAA or 20% PVP, revealing the superiority of PAA in maintaining KTZ in solution. The dissolution enhancement for the PHEMA ASDs, however, did not change significantly, with increasing polymer content.

Crystallization in Aqueous Buffer. Crystallization of the samples in aqueous environment was also evaluated. Each powder sample was wetted with buffer (pH 7.4) and monitored with synchrotron radiation as a function of time. Representative diffraction patterns are shown in Figure 6a−c,

https://dx.doi.org/10.1021/acs.molpharmaceut.0c00790
Mol. Pharmaceutics XXXX, XXX, XXX−XXX

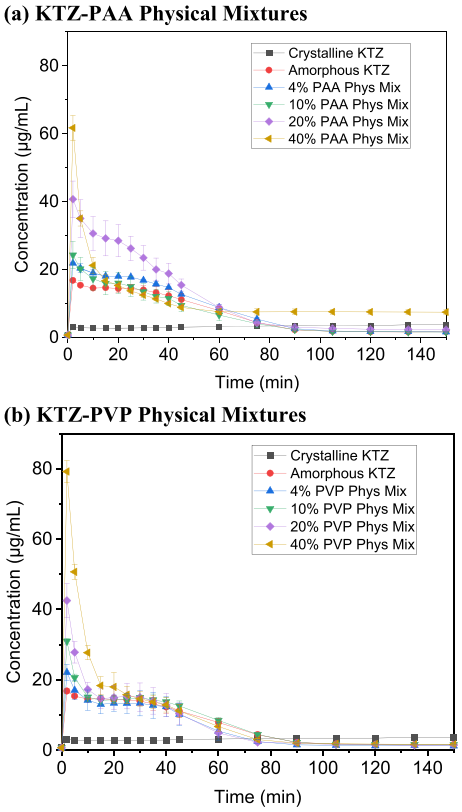

Figure 4. Dissolution profiles of crystalline KTZ, amorphous KTZ, and physical mixtures formulated with (a) PAA and (b) PVP at polymer contents ranging between 4 and 40% w/w (mean ± standard dev; $n = 3$). Experiments were performed in pH 7.4 phosphate buffer at 37 °C. Profiles of KTZ−PHEMA physical mixtures are presented in the Supporting Information (Figure S2b).

from which the extent of crystallization was quantified (Figure 6d). Even at the very low polymer content of 4% w/w, the PAA and PHEMA ASDs were resistant to drug crystallization with less than 12% crystalline content by 4 h. The PVP ASD, on the other hand, crystallized rapidly (~90% crystalline content at 4 h), with the rate of drug crystallization being very similar to that of neat amorphous ketoconazole. Similar results were obtained for ASDs having higher (10 and 20%) polymer contents, where drug crystallization was absent in the PAA and PHEMA ASDs even beyond 4 h, but the PVP ASDs crystallized (data not shown).

When the drug−polymer physical mixtures were evaluated (see Figure 6d), PAA was more effective than PHEMA in inhibiting drug crystallization in solution, even though, for both polymers, the extent of suppression was much less than in the corresponding ASD. PVP, however, did not suppress drug crystallization as a physical mixture.

The crystallization inhibition results complement the observations from the dissolution tests in that PAA and PHEMA were better at stabilizing the drug than PVP. For the water-soluble polymers (PAA and PVP), strong drug−polymer interactions that persist in solution would possibly prevent the dissolved drug from crystallizing and thereby contribute to sustaining the level of supersaturation. For ASDs formulated with hydrogels (e.g., PHEMA), however, the diffusion-controlled drug release mechanism would be more relevant in sustaining supersaturation.

Drug−Polymer Interactions in Solution. The potential interactions between KTZ and the water-soluble polymers, PAA and PVP, were investigated with solution proton NMR spectroscopy as well as isothermal titration calorimetry. The low solubility of PHEMA in water resulted in weak signals, which made it impossible to investigate KTZ−PHEMA interactions. NMR spectra of the drug and polymers are described using the numbering scheme in Figure 1.

1D ^{1}H NMR. Figure 7a shows spectra of the KTZ−polymer mixtures as well as the individual components. Peak assignments for the relevant KTZ protons are listed in Table S1. Peaks of KTZ protons were observed at chemical shifts of ~2 ppm (*N*-acetyl methyl protons), 3−5 ppm (piperazine, dioxolane, and other aliphatic protons), 6−8 ppm (imidazolyl

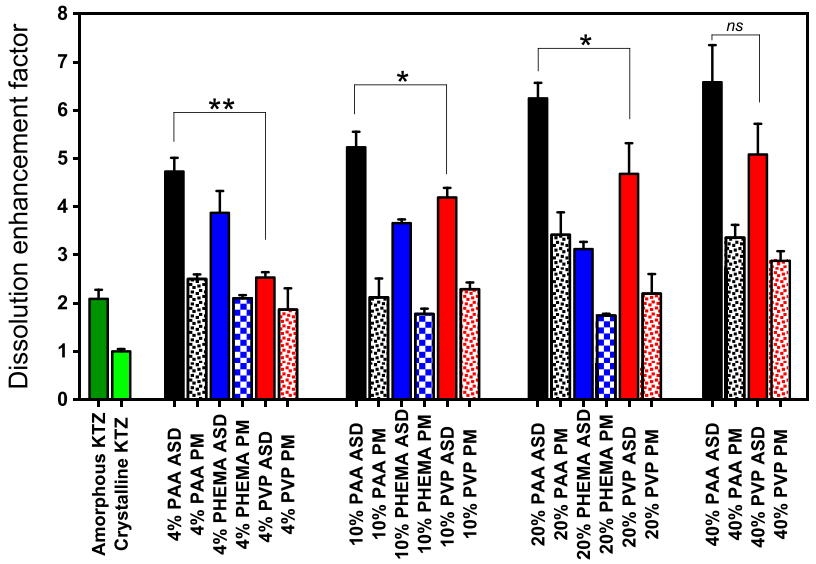

Figure 5. Dissolution enhancement factors obtained from dissolution profiles of amorphous solid dispersions (ASDs) and physical mixtures (PMs) prepared with different polymers (PAA, PHEMA, or PVP) at polymer contents ranging between 4 and 40% w/w. Enhancement factors of crystalline and amorphous KTZ are included for comparison. Student's *t*-test performed between selected ASDs at the same polymer loading: $^{ns}p > 0.05$, $^{*}p \leq 0.05$, $^{**}p \leq 0.01$.

https://dx.doi.org/10.1021/acs.molpharmaceut.0c00790
Mol. Pharmaceutics XXXX, XXX, XXX−XXX

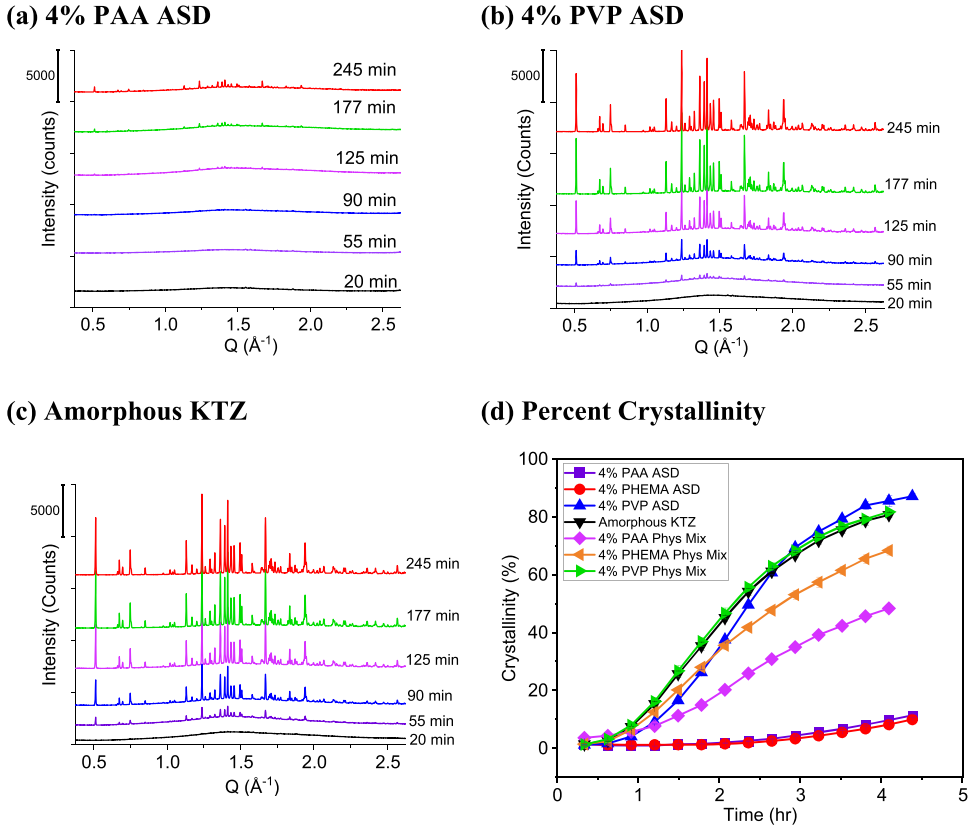

Figure 6. (a–c) Synchrotron X-ray diffraction patterns of powder samples wetted with dissolution medium (phosphate buffer, pH 7.4 at ~25 °C) and monitored as a function of time: (a) KTZ + 4% PAA ASD, (b) KTZ + 4% PVP ASD, and (c) neat amorphous KTZ. Each pattern has been offset on the vertical axis for clarity. (d) Percent crystallinity as a function of time (mean ± SD; n = 3).

and phenyl groups), and >8 ppm (single resonance from the dichlorophenyl ring). The aliphatic proton peaks for neat PAA were between 1 and 3 ppm. The peak corresponding to the carboxylic acid proton of PAA, expected at ~12 ppm, did not appear because of the rapid hydrogen–deuterium exchange in D_2O. The spectrum of neat PVP showed the peaks of the vinyl backbone and the pyrrolidone functional group (1.5–4 ppm). The spectral region between 6 and 9 ppm of both polymers, PAA and PVP, had no peaks and could therefore be used to characterize the behavior of KTZ in the presence of either polymer (see the highlighted area in Figure 7a).

In the presence of PAA, some of the peaks from the aromatic ring systems of KTZ shifted downfield (Figure 7b; red dashed arrows). The most pronounced shifts were observed for the protons of the para-substituted phenyl ring of KTZ (H21/25 in Figure 1a), which moved from 7.06 to 7.35 ppm in the presence of PAA. The peaks assigned to protons of the imidazole group (H10, H12, and H13) also shifted downfield. Since neat KTZ was dissolved under acidic conditions (D_2O at pH 2.5), the basic nitrogen sites (N11 and N26) were protonated (see Figure 1a and the green profile of Figure S1b). Yet, strong peak shifts were still observed, reflecting decreases in the electron densities around the hydrogen atoms, most likely induced by the electron-withdrawing carboxylic acids of PAA.[25,26] In many host–guest complexation systems, peak shifts of 0.1–0.5 ppm typically indicate strongly interacting systems.[26] Thus, both ion–dipole interactions between the positively charged NH groups of KTZ and the carboxylic acids of PAA as well as hydrogen bonding between the oxygen atoms of KTZ (O19 or O34) and the carboxylic acid hydrogens of PAA may be present. The 1D results therefore provided the first indication of interaction between PAA and KTZ in aqueous solution. On the other hand, the KTZ proton peaks in the 6–9 ppm region remained unaffected by the presence of PVP (Figure 7b, green dashed arrows).

2D ^{1}H^{1}H NOESY. Two-dimensional (2D) nuclear Overhauser effect spectroscopy (NOESY) was used to probe the drug–polymer interactions in greater detail. Generally, for small molecules (M_w < 600 Daltons), a nuclear Overhauser effect (NOE) may be observed between protons that are less than 4 Å apart; for large molecules (M_w > ~1500 Daltons), NOEs are observed when the protons are 5 Å apart.[51,52] The sign (or the phase) of the NOE is also related to Brownian motion. In the free state, small molecules tumble rapidly in solution, giving positive NOEs. Conversely, large molecules tumble slowly, showing negative NOEs.[51,52] Thus, the observation of negative NOEs for a small molecule, in the presence of a macromolecule, provides a clear indication of interaction.

The 2D NOESY plot of neat KTZ in D_2O (at pH 2.5) is shown in Figure 8. Several off-diagonal peaks with positive signs (red) are observed, arising from cross-correlations between protons of the drug molecules. Of note, the diagonal peaks are negatively phased (blue). The plot of neat KTZ can be contrasted with those of neat PAA and PVP shown in Figure S4, which have cross-correlations, same-phased with the diagonal peaks. The controls confirm that neat KTZ tumbles rapidly while the neat polymers tumble slowly, as expected.

Figure 9 is the 2D NOESY spectrum of the KTZ–PAA mixture. Cross peaks (circled in red for clarity) between the

https://dx.doi.org/10.1021/acs.molpharmaceut.0c00790
Mol. Pharmaceutics XXXX, XXX, XXX–XXX

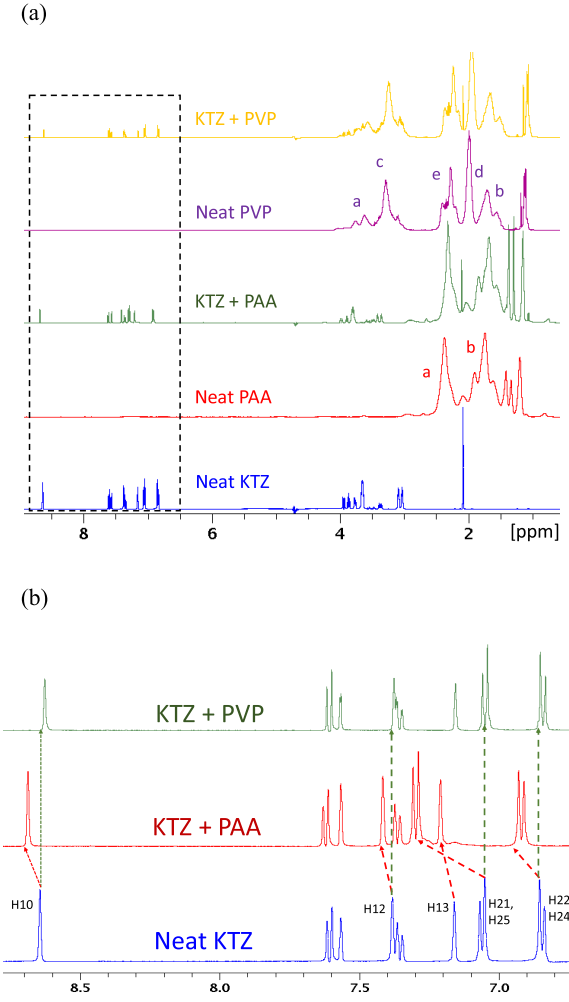

Figure 7. One-dimensional ^{1}H NMR spectra KTZ alone and with polymers in D_2O at pH 2.5. (a) Overview of the entire chemical shift range. The (6.5 to 8.8 ppm) region indicated by a dashed box is expanded in panel (b). Peak position changes for selected KTZ resonances caused by the polymer have been pointed out with dashed arrows.

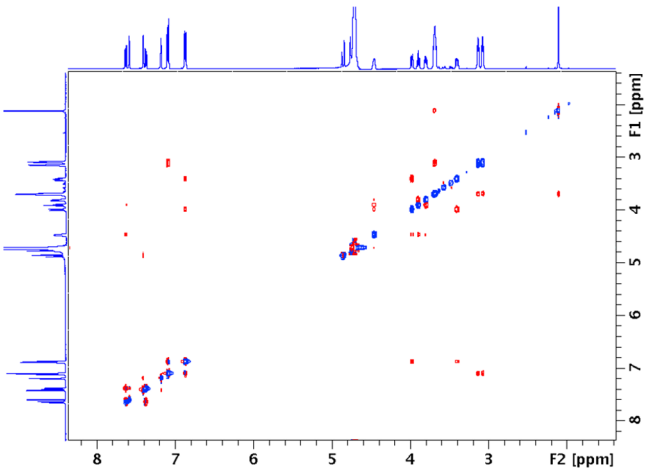

Figure 8. 2D $^{1}H^{1}H$ NOESY plot of KTZ alone in D_2O at pH 2.5. The drug−drug, off-diagonal cross-peaks are red, indicating that they are opposite-phased to the diagonal (blue) peaks.

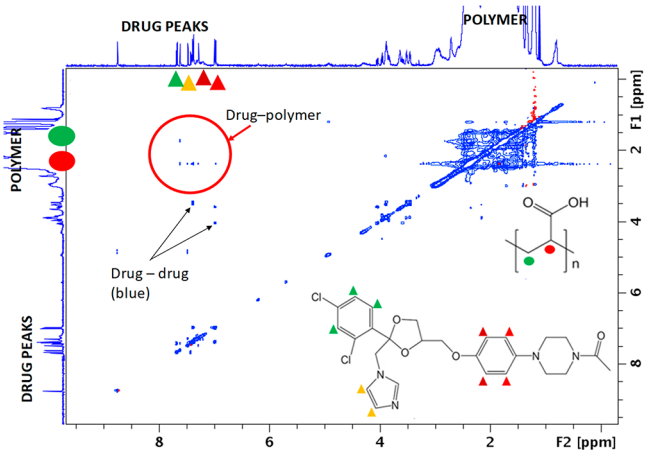

Figure 9. 2D $^{1}H^{1}H$ NOESY plot of a mixture of KTZ and PAA in D_2O. Cross peaks (circled in red) between the aromatic proton peaks of KTZ and the aliphatic proton peaks of PAA indicate drug−polymer intermolecular interactions. All (off-diagonal) cross peaks are blue, same-phased with the diagonal peaks.

aromatic proton peaks of KTZ (H21/25 & H22/24; H12, 13; H3, 5, 6) and those of the aliphatic backbone of PAA (Ha, and to a lesser extent, Hb) indicate the spatial proximity of the KTZ and PAA molecules. The cross peaks have the same phase as the diagonal peaks (negative; blue, in the color scheme), indicating that, in the presence of PAA, the tumbling of the drug molecules is reduced. These results collectively suggest that the polymer and drug molecules are intercalated.

It should be noted that dipolar cross correlations only reflect the spatial proximity of protons. Thus, it is not possible based on the NOESY spectra alone to unequivocally identify the functional groups of the drug and polymer that interact. Since the aliphatic backbone of PAA is spatially close to the aromatic regions of KTZ, hydrophobic drug−polymer associations may be present. It is also possible that the interaction occurs between the imidazole nitrogen of KTZ and the carboxylic acid of PAA but result in the hydrophobic regions being close to each other and manifesting as cross peaks.

In contrast, no cross peaks are observed between the protons of KTZ and PVP (Figure 10). Instead, only intramolecular (i.e., drug−drug or polymer−polymer) cross-correlations are observed. Moreover, the drug−drug and the polymer−polymer cross peaks maintain their positive (red; compare with Figure 8) and negative (blue; compare with Figure S4b) phases, respectively, indicating that the tumbling of KTZ molecules is unaffected by PVP.

2D ^{1}H DOSY. 2D ^{1}H NMR diffusion ordered spectroscopy (DOSY) is another useful tool for investigating molecular interactions in solution.[26,53] The technique enables spectroscopic "separation" of the diffusion coefficients of individual components of a mixture. Small-molecule drugs diffuse faster than bulky polymers.[26] Interaction of the drug with the polymer should, in principle, result in reduced drug diffusivity. However, such an interaction should have a negligible effect on the polymer diffusion coefficient because of the bulky nature of the polymer. The change in the self-diffusion coefficient of the small molecule is thus considered a direct measure of molecular association and aggregation.[26,53,54]

Representative 2D DOSY plots of the drug−polymer mixtures and the controls (KTZ alone, PAA alone, and PVP alone), all prepared in D_2O at pH 2.5, are presented in the

https://dx.doi.org/10.1021/acs.molpharmaceut.0c00790
Mol. Pharmaceutics XXXX, XXX, XXX−XXX

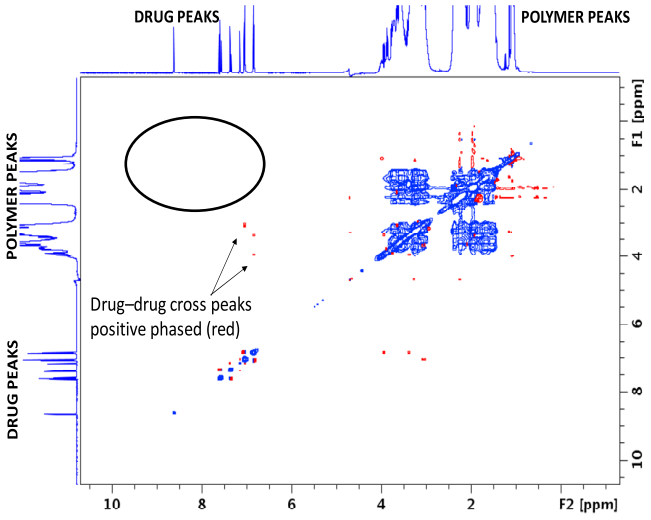

Figure 10. 2D $^{1}H^{1}H$ NOESY plot of a mixture of KTZ and PVP in D_2O at pH 2.5. No drug–polymer cross peaks are observed in the circled region. Only drug–drug (red; some pointed out) or polymer–polymer (blue) cross peaks can be identified.

Supporting Information (Figure S5). The corresponding diffusion coefficient values (D values) are listed in Table S2. The diffusion coefficient of KTZ alone, 3.5×10^{-10} m^2 s^{-1}, is in good agreement with the values of other similar small-molecule drugs in D_2O.[55,56] The neat polymers, PAA and PVP, have similar diffusion values ($\sim 1.7 \times 10^{-10}$ m^2 s^{-1}), reflecting the similarity in their molecular weights and shape (1800 and 2500 g/mol for PAA and PVP, respectively, both linear with ~24 monomers per chain). The polymer diffusion values are also consistent with the literature.[25,38]

To gauge the magnitude of the influence of the drug–polymer interaction on the movement of the different species in solution, the measured D values are normalized with the D value of neat KTZ (D_0). The resulting (D/D_0) values are presented in Figure 11 with the neat drug having a value of 1

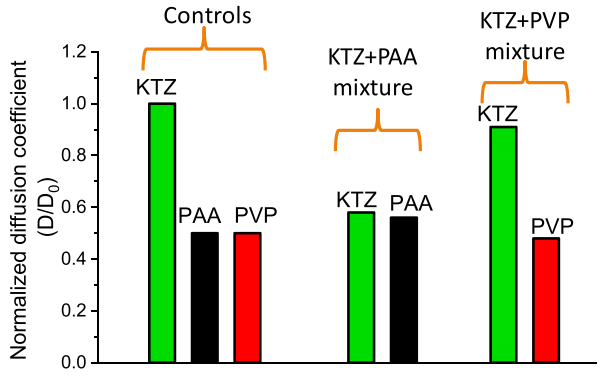

Figure 11. Normalized diffusion coefficients of the neat drug (KTZ alone), neat polymers (PAA or PVP alone), and the drug or polymer in the drug–polymer mixtures.

and the neat polymers having values of ~0.5. In the presence of PAA, the normalized D value of KTZ is ~0.58, indicating that the drug movement is slowed down by the polymer. The extent of reduction of drug diffusivity in the polymer solution is likely correlated with solubility enhancement due to the polymer.[56] In the presence of PVP, however, the diffusion coefficient of KTZ is similar to that of the neat drug (D/D_0 = 0.91), indicating that the polymer has a negligible effect on drug diffusion and further corroborating the absence of drug–polymer interactions. As expected, the diffusivity of PAA or PVP, in the respective drug–polymer mixtures, remains unchanged, as compared to the neat polymers.

Isothermal Titration Calorimetry (ITC). Figure 12a shows the raw ITC power compensation signals for the

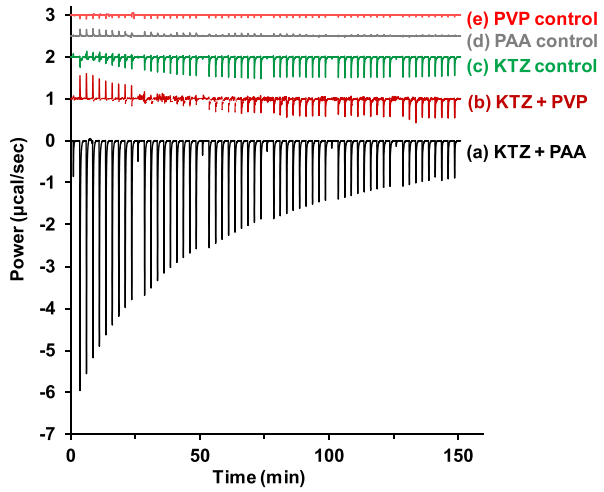

Figure 12. Isothermal titration calorimetry power compensation signals obtained from sequential injections of (a) 40 mM KTZ into 3 mM PAA, (b) 40 mM KTZ into 3 mM PVP, (c) 40 mM KTZ into plain buffer (pH 1.1), (d) plain buffer into 3 mM PAA, and (e) plain buffer into 3 mM PVP. For clarity, b, c, d, and e have been offset by 1, 2, 2.5, and 3 units, respectively, on the vertical axis.

titration of KTZ into PAA. An exothermic signal of ~6 μcal/s is initially registered. The magnitudes of the peaks progressively decrease with sequential titration of drug into polymer solution until the end of the experiments, when the signal is ~1 μcal/s. A separate control experiment, comprising titration of KTZ into the blank solvent (pH 1.1 buffer), was performed (labeled as KTZ control; Figure 12c) to obtain the dilution heats, which are of a much smaller magnitude. The pH values of the drug solution, the polymer solutions, and blank buffer were within 0.2 units of each other. The drug dilution heats observed are therefore not attributed to a mismatch in pH of the syringe and cell contents but presumably from the entropic gain when drug molecules from the highly concentrated syringe solution spread through the buffer in the sample cell. The drug dilution background heats could also indicate some form of aggregation such as dimerization of the drug molecules in solution, even though this is not expected in the case of ketoconazole. In a second blank experiment, the heat of dilution of the polymer was also measured by titrating buffer from the syringe into the polymer solution in the sample cell (labeled as PAA control; Figure 12d). The heats of dilution of both polymer solutions, measured in this way, are negligible.

The peaks recorded following each stepwise injection of KTZ into PAA were integrated, normalized with respect to the moles of drug added per injection, and then plotted as a function of the drug-to-polymer molar ratio in the sample cell. This representation is commonly referred to as the differential binding curve (Figure 13a). The shape of the curve obtained for the titration of KTZ into PAA is typical for binding interactions with weak affinity ($K_a < 10^4$ M^{-1}).[34,57] Similar profiles have been reported for drug–cyclodextrin interac-

https://dx.doi.org/10.1021/acs.molpharmaceut.0c00790
Mol. Pharmaceutics XXXX, XXX, XXX−XXX

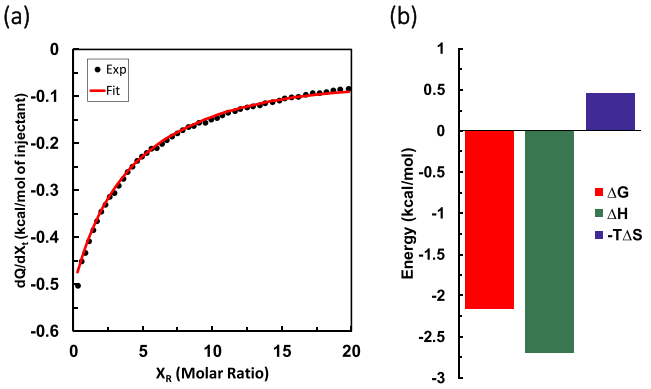

Figure 13. Isothermal titration calorimetry results. (a) Integrated heat as a function of drug-to-polymer molar ratio for the titration of 40 mM KTZ into 3 mM PAA. The standard one-set-of-sites binding model was fitted to the experimental data (exp). (b) "Binding" signature plot (overall change in free energy, enthalpy, and entropy factor) for the KTZ−PAA titration.

tions[58] as well as protein−carbohydrate interactions.[59] In standard practice, a thermodynamic binding model is fitted to the differential binding data to provide additional insight into the ligand−macromolecular interaction mechanism.[60] A good fit was obtained using an independent site analysis approach, with one independent set of sites and an additional term that accounts for the contribution from drug dilution (see the Supporting Information).[35,60] The stoichiometry parameter, *n*, was fixed to 1, an approach that can be used for analyzing data with weak binding affinity to increase the confidence in the other fit parameters.[57,61,62] The resulting fit to the binding isotherm is shown in Figure 13a, and the corresponding thermodynamic binding signature is plotted in Figure 13b. The data analysis shows an association constant (K_a) of 43.3 ± 0.4 M^{-1}, with a negative overall enthalpy change (ΔH = −2.69 ± 0.02 kcal/mol) indicating an enthalpy-driven interaction. The enthalpic contribution from the drug dilution is negligible ($\Delta H_{dil} \approx 0.1$ kcal/mol).

The overall enthalpy change extracted from ITC experiments provides a measure of the energy content of bonds broken and formed in the interaction process. In general, polar interactions tend to contribute favorably to the enthalpic component, the major contribution being from hydrogen bonds, whereas entropically favored interactions tend to be more hydrophobic. Thus, the binding signature suggests polar interactions such as hydrogen bonding or ion−dipole interactions, most likely between the imidazole groups of KTZ and the carboxylic acids of PAA being present. The interaction is spontaneous and favorable due to the negative change in free energy (ΔG = −2.3 kcal/mol).

The ITC profile obtained for the titration of KTZ into PVP (Figure 12b), however, starts with very weak endothermic peaks (~0.5 μcal/s), which become exothermic when the drug-to-polymer molar ratio is greater than 5. The exothermic signals of the KTZ−PVP interaction are of the same magnitude as the signal for the titration of KTZ into the blank buffer (~0.5 μcal/s). Subtraction of the heat of KTZ dilution, from the KTZ−PVP titration, results in a largely featureless differential enthalpy curve, which cannot be fitted with any of the standard binding models.

Possible Mechanisms of Interaction in Aqueous Solution. Together, the NMR and ITC experiments clearly show that interactions between KTZ and PAA exist in aqueous solution, which are stronger than interactions, if any, between KTZ and PVP. Because KTZ is weakly basic, with ionizable functional groups, the ionization states of both the drug and the polymer will influence the type of interaction occurring in aqueous solution. In acidic buffer (<pH 2.5), the imidazolyl group of KTZ is fully protonated assuming a net positive charge, whilst the carboxylic acids of PAA (pKa ≈ 4.5), though protonated, remain uncharged. In neutral medium where the dissolution experiments were conducted, the charges are reversed; KTZ becomes substantially neutral (~10% protonated), while PAA gains a net negative charge due to deprotonation of the carboxylic acid groups. Thus, in either acidic or neutral medium, ion−dipole interactions between the drug and polymer would very likely be present. Additionally, multiple avenues exist for hydrogen bonding between KTZ and PAA, which could contribute to the overall interaction strength. The thermodynamic interaction signature from the ITC experiments also point to enthalpy-driven, polar interactions being dominant. It is therefore reasonable to infer that strong interactions in the solid state translate to aqueous solution, explaining, at least in part, the sustained duration of supersaturation in the dissolution experiments.

It is noteworthy that the KTZ−PAA ASDs outperformed the KTZ−PVP ASDs when the polymer contents were low (4−20% w/w polymer); at 40% polymer content, the dissolution profiles of the ASDs, regardless of polymer type, were not statistically different (see Figure 5). This suggests that for water-soluble polymers, the strong drug−polymer interactions may contribute substantially to sustaining the level of supersaturation at low polymer contents. Other factors such as steric hindrance to precipitation, due to the bulkiness of the polymer, become equally important at higher polymer contents.

Finally, we will briefly address the relevance of our work to the *in vivo* situation, specifically following oral administration. We will consider KTZ−PAA as the model system. The highly acidic gastric fluid will favor the solubility of KTZ. As the dissolved ASD transitions to the intestine, drug crystallization would likely be prevented if the drug−polymer interaction persists. Even though soluble drug−polymer complexes can, in principle, inhibit release of free drug, the low association constant (K_a) obtained for the KTZ−PAA system suggests that drug release and subsequent drug absorption would not be inhibited.

■ SIGNIFICANCE

This study provides mechanistic insights into the factors that affect the dissolution of ASDs, providing a basis for rational polymer selection. When a polymer that can form strong (e.g., ionic) interactions with the drug is selected, stable ASDs can be prepared at low polymer loadings. This could accomplish multiple goals of (i) reducing the pill burden, (ii) preventing solid-state drug crystallization in the dosage form, and (iii) improving the dissolution performance of the ASDs. To determine the extent of generalizability of the hypothesis, a wider range of drug−polymer systems needs to be studied. We have noticed from our ongoing studies that other techniques that can provide complementary information on interaction patterns in aqueous solution will likely be required because of the challenge posed by the poor aqueous solubility of the model drugs.[63] The next step would be to investigate if the dissolution enhancement observed *in vitro* due to strong interactions translates to enhanced bioavailability *in vivo*.

https://dx.doi.org/10.1021/acs.molpharmaceut.0c00790
Mol. Pharmaceutics XXXX, XXX, XXX−XXX

CONCLUSIONS

In our earlier work, we showed that strong interactions (ionic as well as hydrogen bonding) between ketoconazole (KTZ) and poly(acrylic acid) (PAA) resulted in pronounced reduction in both the molecular mobility and the crystallization propensity of the amorphous solid dispersion (ASD) in the dry, "solid" state. Weak dipole−dipole interactions between KTZ and polyvinylpyrrolidone (PVP) however resulted in an ASD that crystallized more rapidly. In this work, using 2D nuclear Overhauser effect spectroscopy, diffusion ordered spectroscopy, and isothermal titration calorimetry, we demonstrated the existence of KTZ−PAA interactions in aqueous solution. The solution-state interaction translated to prolonged duration of supersaturation, reflecting resistance to drug crystallization in aqueous media. Conversely, no evidence of KTZ−PVP interactions was observed in aqueous solution. The sustainment of supersaturation with PVP was much less pronounced. The results suggest that, in this system, and possibly for other weakly basic drugs, the interactions that stabilize ASDs in the solid state can also be relevant and important in sustaining the level of supersaturation in solution.

ASSOCIATED CONTENT

Supporting Information

The Supporting Information is available free of charge at https://pubs.acs.org/doi/10.1021/acs.molpharmaceut.0c00790.

Solubility and microspecies distribution profiles of ketoconazole as a function of pH, dissolution profiles of ketoconazole−PHEMA amorphous solid dispersions and physical mixtures, plots of maximum dissolved drug concentration and total dissolved drug obtained from dissolution profiles, one-dimensional NMR peak assignments, additional two-dimensional NOESY and DOSY spectra, and isothermal titration calorimetry data analysis background information (PDF)

AUTHOR INFORMATION

Corresponding Author

Raj Suryanarayanan − *Department of Pharmaceutics, College of Pharmacy, University of Minnesota, Minneapolis, Minnesota 55455, United States;* orcid.org/0000-0002-6322-0575; Email: surya001@umn.edu

Authors

Kweku K. Amponsah-Efah − *Department of Pharmaceutics, College of Pharmacy, University of Minnesota, Minneapolis, Minnesota 55455, United States*

Pinal Mistry − *Department of Pharmaceutics, College of Pharmacy, University of Minnesota, Minneapolis, Minnesota 55455, United States*

Reed Eisenhart − *Department of Chemistry, University of Minnesota, Minneapolis, Minnesota 55455, United States*

Complete contact information is available at: https://pubs.acs.org/10.1021/acs.molpharmaceut.0c00790

Notes

The authors declare no competing financial interest.

ACKNOWLEDGMENTS

This project was funded by the National Science Foundation (grant number NSF-CMMI-1662046) and partially supported by the William and Mildred Peters endowment fund. K.K.A.E. acknowledges the Bighley Graduate Student Fellowship. The research used resources of the Advanced Photon Source, a U.S. Department of Energy (DOE) Office of Science User Facility, operated for the DOE Office of Science by Argonne National Laboratory, under contract number DE-AC02-06CH11357. Dr. Wenquian Hu and Dr. Andrey Yakovenko (beamline 17-BM-B) are acknowledged for their help. The authors are grateful to Dr. Courtney Aldrich, University of Minnesota, for granting access to an ITC-200 microcalorimeter (NIH shared instrumentation grant S10-OD017982) and Dr. Anant Paradkar, University of Bradford, for granting access to a USP dissolution apparatus IV. We also thank Dr. Letitia Yao (NMR), Dr. Michelle Miller (NMR), Evan Alexander (ITC), and Dr. Shivprasad Deshmukh (dissolution tests) for their help with experiments and Dr. Eva Munoz and Dr. Juan Sabin for their help with fitting of the ITC data.

REFERENCES

(1) Newman, A.; Knipp, G.; Zografi, G. Assessing the performance of amorphous solid dispersions. *J. Pharm. Sci.* **2012**, *101*, 1355−1377.

(2) Lipinski, C. A.; Lombardo, F.; Dominy, B. W.; Feeney, P. J. Experimental and Computational Approaches to Estimate Solubility and Permeability in Drug Discovery and Development Settings. *Adv. Drug Delivery Rev.* **2001**, *46*, 3−26.

(3) Lipinski, C. A.; Lombardo, F.; Dominy, B. W.; Feeney, P. J. Experimental and computational approaches to estimate solubility and permeability in drug discovery and development settings. *Adv. Drug Delivery Rev.* **1997**, *23*, 3−25.

(4) Butler, J. M.; Dressman, J. B. The developability classification system: Application of biopharmaceutics concepts to formulation development. *J. Pharm. Sci.* **2010**, *99*, 4940−4954.

(5) Baghel, S.; Cathcart, H.; O'Reilly, N. J. Polymeric Amorphous Solid Dispersions : A Review of Amorphization , Crystallization , Stabilization , Solid-State Characterization , and Aqueous Solubilization of Biopharmaceutical Classification System Class II Drugs. *J. Pharm. Sci.* **2016**, *105*, 2527−2544.

(6) Khougaz, K.; Clas, S.-D. Crystallization Inhibition in Solid Dispersions of MK-0591 and Poly(vinylpyrrolidone) Polymers. *J. Pharm. Sci.* **2000**, *89*, 1325−1334.

(7) Grzybowska, K.; Capaccioli, S.; Paluch, M. Recent developments in the experimental investigations of relaxations in pharmaceuticals by dielectric techniques at ambient and elevated pressure. *Adv. Drug Delivery Rev.* **2016**, *100*, 158−182.

(8) Konno, H.; Taylor, L. S. Influence of Different Polymers on the Crystallization Tendency of Molecularly Dispersed Amorphous Felodipine. *J. Pharm. Sci.* **2006**, *95*, 2692−2705.

(9) Shamblin, S. L.; Huang, E. Y.; Zografi, G. The effects of co-lyophilized polymeric additives on the glass transition temperature and crystallization of amorphous sucrose. *J. Therm. Anal.* **1996**, *47*, 1567−1579.

(10) Wellscheid, R.; Wüst, J.; Jungnickel, B.-J. The competition between crystallization and demixing in polymer blends. IV. Detection of composition inhomogeneities around growing spherulites. *J. Polym. Sci., Part B: Polym. Phys.* **1996**, *34*, 267−275.

(11) Kalivianakis, P.; Jungnickel, B. J. Crystallization-induced composition inhomogeneities in PVDF/PMMA blends. *J. Polym. Sci., Part B: Polym. Phys.* **1998**, 2923.

(12) Yang, Z.; Han, C. D. Rheology of Miscible Polymer Blends with Hydrogen Bonding. *Macromolecules* **2008**, *41*, 2104−2118.

(13) Mistry, P.; Mohapatra, S.; Gopinath, T.; Vogt, F. G.; Suryanarayanan, R. Role of the Strength of Drug−Polymer Interactions on the Molecular Mobility and Crystallization Inhibition in Ketoconazole Solid Dispersions. *Mol. Pharmaceutics* **2015**, *12*, 3339−3350.

(14) Song, Y.; Yang, X.; Chen, X.; Nie, H.; Byrn, S.; Lubach, J. W. Investigation of Drug-Excipient Interactions in Lapatinib Amorphous

Solid Dispersions Using Solid-State NMR Spectroscopy. *Mol. Pharmaceutics* **2015**, *12*, 857−866.
(15) Yuan, X.; Xiang, T.-X.; Anderson, B. D.; Munson, E. J. Hydrogen Bonding Interactions in Amorphous Indomethacin and its Amorphous Solid Dispersions with Poly(vinylpyrrolidone) and Poly(vinylpyrrolidone-co-vinyl acetate) Studied using (13)C Solid-State NMR. *Mol. Pharmaceutics* **2015**, *12*, 4518−4528.
(16) Matsumoto, T.; Zografi, G. Physical properties of solid molecular dispersions of indomethacin with poly(vinylpyrrolidone) and poly(vinylpyrrolidone-co-vinyl-acetate) in relation to indomethacin crystallization. *Pharm. Res.* **1999**, *16*, 1722−1728.
(17) Kothari, K.; Ragoonanan, V.; Suryanarayanan, R. The role of drug-polymer hydrogen bonding interactions on the molecular mobility and physical stability of nifedipine solid dispersions. *Mol. Pharmaceutics* **2015**, *12*, 162−170.
(18) Van Eerdenbrugh, B.; Taylor, L. S. Application of mid-IR spectroscopy for the characterization of pharmaceutical systems. *Int. J. Pharm.* **2011**, *417*, 3−16.
(19) Kestur, U. S.; Van Eerdenbrugh, B.; Taylor, L. S. Influence of polymer chemistry on crystal growth inhibition of two chemically diverse organic molecules. *CrystEngComm* **2011**, *13*, 6712−6718.
(20) Chen, Y.; Wang, S.; Wang, S.; et al. Initial Drug Dissolution from Amorphous Solid Dispersions Controlled by Polymer Dissolution and Drug-Polymer Interaction. *Pharm. Res.* **2016**, *33*, 2445−2458.
(21) Saboo, S.; Kestur, U. S.; Flaherty, D. P.; Taylor, L. S. Congruent Release of Drug and Polymer from Amorphous Solid Dispersions: Insights into the Role of Drug-Polymer Hydrogen Bonding, Surface Crystallization, and Glass Transition. *Mol. Pharmaceutics* **2020**, 1261.
(22) Mistry, P.; Suryanarayanan, R. Strength of Drug−Polymer Interactions: Implications for Crystallization in Dispersions. *Cryst. Growth Des.* **2016**, *16*, 5141−5149.
(23) Ueda, K.; Higashi, K.; Yamamoto, K.; Moribe, K. Inhibitory effect of hydroxypropyl methylcellulose acetate succinate on drug recrystallization from a supersaturated solution assessed using nuclear magnetic resonance measurements. *Mol. Pharmaceutics* **2013**, *10*, 3801−3811.
(24) Morris, K. F.; Johnson, C. S. Diffusion-ordered two-dimensional nuclear magnetic resonance spectroscopy. *J. Am. Chem. Soc.* **1992**, *114*, 3139−3141.
(25) Hädener, M.; Gjuroski, I.; Furrer, J.; Vermathen, M. Interactions of Polyvinylpyrrolidone with Chlorin e6-Based Photosensitizers Studied by NMR and Electronic Absorption Spectroscopy. *J Phys Chem B.* **2015**, *119*, 12117−12128.
(26) Fielding, L. Determination of Association Constants (Ka) from Solution NMR Data. *Tetrahedron* **2000**, *56*, 6151−6170.
(27) Li, Z.; Johnson, L. M.; Ricarte, R. G.; et al. Enhanced Performance of Blended Polymer Excipients in Delivering a Hydrophobic Drug through the Synergistic Action of Micelles and HPMCAS. *Langmuir* **2017**, *33*, 2837−2848.
(28) Arnaud, A.; Bouteiller, L. Isothermal titration calorimetry of supramolecular polymers. *Langmuir* **2004**, *20*, 6858−6863.
(29) Mistry, P.; Amponsah-Efah, K. K.; Suryanarayanan, R. Rapid Assessment of the Physical Stability of Amorphous Solid Dispersions. *Cryst. Growth Des.* **2017**, *17*, 2478−2485.
(30) Nunes, C.; Mahendrasingam, A.; Suryanarayanan, R. Quantification of crystallinity in substantially amorphous materials by synchrotron X-ray powder diffractometry. *Pharm. Res.* **2005**, *22*, 1942−1953.
(31) Whitehouse, L. W.; Menzies, A.; Dawson, B.; et al. Mouse hepatic metabolites of ketoconazole: Isolation and structure elucidation. *J. Pharm. Biomed. Anal.* **1994**, *12*, 1425−1441.
(32) Redenti, E.; Ventura, P.; Fronza, G.; et al. Experimental and theoretical analysis of the interaction of (±)-cis- ketoconazole with β-cyclodextrin in the presence of (+)-L-tartaric acid. *J. Pharm. Sci.* **1999**, *88*, 599−607.
(33) *Handbook of Proton-Nmr Spectra and Data*. Elsevier; 1987, DOI: 10.1016/B978-0-12-064511-4.50007-5
(34) Freyer, M. W.; Lewis, E. A. Isothermal Titration Calorimetry: Experimental Design, Data Analysis, and Probing Macromolecule/Ligand Binding and Kinetic Interactions. *Methods Cell Biol.* **2008**, *84*, 79−113.
(35) Piñeiro, Á.; Muñoz, E.; Sabín, J.; et al. AFFINImeter: A software to analyze molecular recognition processes from experimental data. *Anal. Biochem.* **2019**, *577*, 117−134.
(36) Dressman, J. B.; Reppas, C. In vitro-in vivo correlations for lipophilic, poorly water-soluble drugs. *Eur. J. Pharm. Sci.* **2000**, *11*, S73−S80.
(37) Paterson, S. M.; Brown, D. H.; Chirila, T. V.; Keen, I.; Whittaker, A. K.; Baker, M. V. The synthesis of water-soluble PHEMA via ARGET ATRP in protic media. *J. Polym. Sci., Part A Polym. Chem.* **2010**, *48*, 4084−4092.
(38) Swift, T.; Swanson, L.; Geoghegan, M.; Rimmer, S. The pH-responsive behaviour of poly(acrylic acid) in aqueous solution is dependent on molar mass. *Soft Matter* **2016**, *12*, 2542−2549.
(39) Bühler, V. *Kollidon® Polyvinylpyrrolidone Excipients for the Pharmaceutical Industry*; 9th Editio. BASF SE, Pharma Ingredients and Services: 2008, DOI: 10.1016/B978-0-12-802182-8.00001-5
(40) BASF. *Soluble Kollidon ® Grades*; http://www.pharma-ingredients.basf.com/Statements/Technical Informations/EN/Pharma Solutions/03_030730e_Soluble Kollidon grades.pdf.
(41) Lubach, J. W.; Chen, J. Z.; Hau, J.; et al. Investigation of the rat model for preclinical evaluation of pH-dependent oral absorption in humans. *Mol. Pharmaceutics* **2013**, *10*, 3997−4004.
(42) Ilevbare, G. A.; Taylor, L. S. Liquid-liquid phase separation in highly supersaturated aqueous solutions of poorly water-soluble drugs: Implications for solubility enhancing formulations. *Cryst. Growth Des.* **2013**, *13*, 1497−1509.
(43) Babu, N. J.; Nangia, A. Solubility Advantage of Amorphous Drugs and Pharmaceutical Cocrystals. *Cryst. Growth Des.* **2011**, *11*, 2662−2679.
(44) Guzmán, H. R.; Tawa, M.; Zhang, Z.; et al. Combined Use of Crystalline Salt Forms and Precipitation Inhibitors to Improve Oral Absorption of Celecoxib from Solid Oral Formulations. *J. Pharm. Sci.* **2007**, *96*, 2686−2702.
(45) Fung, M.; Bērziņš, K.; Suryanarayanan, R. Physical Stability and Dissolution Behavior of Ketoconazole−Organic Acid Coamorphous Systems. *Mol. Pharmaceutics* **2018**, *15*, 1862−1869.
(46) Sun, D. D.; Lee, P. I. Probing the mechanisms of drug release from amorphous solid dispersions in medium-soluble and medium-insoluble carriers. *J. Controlled Release* **2015**, *211*, 85−93.
(47) Sun, D. D.; Ju, T. R.; Lee, P. I. Enhanced kinetic solubility profiles of indomethacin amorphous solid dispersions in poly(2-hydroxyethyl methacrylate) hydrogels. *Eur. J. Pharm. Biopharm.* **2012**, *81*, 149−158.
(48) Zahedi, P.; Lee, P. I. Solid molecular dispersions of poorly water-soluble drugs in poly(2-hydroxyethyl methacrylate) hydrogels. *Eur. J. Pharm. Biopharm.* **2007**, *65*, 320−328.
(49) Doherty, C.; York, P. Mechanisms of dissolution of frusemide/PVP solid dispersions. *Int. J. Pharm.* **1987**, *34*, 197−205.
(50) Chiou, W. L.; Riegelman, S. Pharmaceutical Applications of Solid Dispersion Systems. *J. Pharm. Sci.* **1971**, *60*, 1281−1302.
(51) Butts, C. P.; Jones, C. R.; Towers, E. C.; Flynn, J. L.; Appleby, L.; Barron, N. J. Interproton distance determinations by NOE−surprising accuracy and precision in a rigid organic molecule. *Org. Biomol. Chem.* **2011**, *9*, 177−184.
(52) Macura, S.; Ernst, R. R. Elucidation of cross relaxation in liquids by two-dimensional N.M.R. spectroscopy. *Mol. Phys.* **2002**, *100*, 135−147.
(53) Cohen, Y.; Avram, L.; Frish, L. Diffusion NMR spectroscopy in supramolecular and combinatorial chemistry: An old parameter - New insights. *Angew. Chem., Int. Ed.* **2005**, *44*, 520−554.
(54) Cameron, K. S.; Fielding, L. NMR Diffusion Spectroscopy as a Measure of Host−Guest Complex Association Constants and as a Probe of Complex Size. *J Org Chem.* **2001**, *66*, 6891−6895.

https://dx.doi.org/10.1021/acs.molpharmaceut.0c00790
Mol. Pharmaceutics XXXX, XXX, XXX−XXX

(55) Ting, J. M.; Tale, S.; Purchel, A. A.; et al. High-Throughput Excipient Discovery Enables Oral Delivery of Poorly Soluble Pharmaceuticals. *ACS Cent. Sci.* **2016**, *2*, 748−755.
(56) Saal, W.; Ross, A.; Wyttenbach, N.; Alsenz, J.; Kuentz, M. A Systematic Study of Molecular Interactions of Anionic Drugs with a Dimethylaminoethyl Methacrylate Copolymer Regarding Solubility Enhancement. *Mol. Pharmaceutics* **2017**, *14*, 1243−1250.
(57) Turnbull, W. B.; Daranas, A. H. On the Value of *c* : Can Low Affinity Systems Be Studied by Isothermal Titration Calorimetry? *J. Am. Chem. Soc.* **2003**, *125*, 14859−14866.
(58) Segura-Sanchez, F.; Bouchemal, K.; Lebas, G.; Vauthier, C.; Santos-Magalhaes, N. S.; Ponchel, G. Elucidation of the complexation mechanism between (+)-usnic acid and cyclodextrins studied by isothermal titration calorimetry and phase-solubility diagram experiments. *J. Mol. Recognit.* **2009**, *22*, 232−241.
(59) Dam, T. K.; Brewer, C. F. Thermodynamic studies of lectin-carbohydrate interactions by isothermal titration calorimetry. *Chem. Rev.* **2002**, *102*, 387−430.
(60) Wiseman, T.; Williston, S.; Brandts, J. F.; Lin, L. N. Rapid measurement of binding constants and heats of binding using a new titration calorimeter. *Anal. Biochem.* **1989**, *179*, 131−137.
(61) Tellinghuisen, J. Optimizing experimental parameters in isothermal titration calorimetry. *J Phys Chem B.* **2005**, *109*, 20027−20035.
(62) Tellinghuisen, J. Isothermal titration calorimetry at very low c. *Anal. Biochem.* **2008**, *373*, 395−397.
(63) Kweku, K.; Amponsah-Efah; Demeler, B.; Suryanarayanan, R. Characterizing Drug-Polymer Interactions in Aqueous Solution with Analytical Ultracentrifugation. *Mol. Pharm.* **2021**. DOI: 10.1021/acs.molpharmaceut.0c00849.

https://dx.doi.org/10.1021/acs.molpharmaceut.0c00790
Mol. Pharmaceutics XXXX, XXX, XXX−XXX